Neuron, Vol. 47, 555–566, August 18, 2005, Copyright ©2005 by Elsevier Inc. DOI 10.1016/j.neuron.2005.06.033

Coassembly of Two GluR6 Kainate Receptor Splice Variants within a Functional Protein Complex

Françoise Coussen,[1] David Perrais,[1] Frédéric Jaskolski,[1] Shankar Sachidhanandam,[1] Elisabeth Normand,[1] Joel Bockaert,[2] Philippe Marin,[2] and Christophe Mulle[1,*]

[1]Laboratoire "Physiologie Cellulaire de la Synapse"
CNRS, UMR 5091
Institut François Magendie
Université Bordeaux
2, rue C. Saint-Saëns
33077 Bordeaux Cedex
France

[2]CNRS, UMR 5203
Inserm U661
34094 Montpellier Cedex
France

Summary

Kainate receptors (KAR) are composed of several distinct subunits and splice variants, but the functional relevance of this diversity remains largely unclear. Here we show that two splice variants of the GluR6 subunit, GluR6a and GluR6b, which differ in their C-terminal domains, do not show distinct functional properties, but coassemble as heteromers in vitro and in vivo. Using a proteomic approach combining affinity purification and MALDI-TOF mass spectrometry, we found that GluR6a and GluR6b interact with two distinct subsets of cytosolic proteins mainly involved in Ca^{2+} regulation of channel function and intracellular trafficking. Guided by these results, we provide evidence that the regulation of native KAR function by NMDA receptors depends on the heteromerization of GluR6a and GluR6b and interaction of calcineurin with GluR6b. Thus, GluR6a and GluR6b bring in close proximity two separate subsets of interacting proteins that contribute to the fine regulation of KAR trafficking and function.

Introduction

Targeting and stabilization of glutamate receptors in specialized neuronal compartments involve interactions with a variety of scaffolding, intracellular trafficking, or signal transduction proteins (Bredt and Nicoll, 2003; Choquet and Triller, 2003; Wenthold et al., 2003). The variety of proteins recently described as interactors of AMPA and NMDA receptors have begun to unravel the cascade of events that leads to the regulation of these receptors at synaptic sites, especially during synaptic plasticity (Barry and Ziff, 2002; Bredt and Nicoll, 2003; Collingridge et al., 2004; Sheng, 2001; Song and Huganir, 2002; Wenthold et al., 2003). Far less is known about ionotropic glutamate receptors of the kainate type (KARs), which play an important role in the regulation of synaptic transmission and neuronal excitability by acting at either presynaptic, postsynaptic, or extrasynaptic sites (Huettner, 2003; Jaskolski et al., 2005; Lerma, 2003). Although the physiological function of KARs critically depends on their specific localization and density in these various neuronal compartments, molecular determinants for the polarized expression of KARs have not yet been characterized.

KARs are hetero-oligomeric receptor channels assembled from the GluR5, GluR6, GluR7, KA1, and KA2 subunits (Bettler and Mulle, 1995; Lerma, 2003). GluR5, GluR6, and GluR7 can function as homomeric recombinant receptor channels, although native KARs are likely to be heteromeric receptors. KA1 and KA2 associate with these subunits to form heteromeric receptors with distinct pharmacological properties. GluR5 and GluR6 also coassemble to generate recombinant receptors with novel functional properties (Cui and Mayer, 1999). Immunoprecipitation experiments and electrophysiological comparison of KAR subunit-deficient mice have indicated that brain KARs are composed of various combinations of subunits. For instance, GluR6, a major KAR channel-forming subunit, assembles with KA2 (Wenthold et al., 1994) in CA3 pyramidal cells (Contractor et al., 2003) and with GluR5 in hippocampal interneurons (Mulle et al., 2000).

The diversity of KARs is increased by the existence of splice variants for GluR5, GluR6, and GluR7 receptor subunits (Bettler and Mulle, 1995; Jaskolski et al., 2005; Lerma, 2003). We have recently shown that subunit composition and splice variants regulate membrane trafficking of KARs (Jaskolski et al., 2004). The C-terminal domains of KA2 and GluR5c carry endoplasmic reticulum (ER) retention signals (Jaskolski et al., 2004; Ren et al., 2003a, 2003b), whereas GluR6a contains a forward trafficking motif necessary for efficient surface expression (Jaskolski et al., 2004; Yan et al., 2004).

Because KAR subunit splice variants differ in their C-terminal domains, their differential trafficking is likely attributable to interactions with distinct subsets of cytoplasmic trafficking proteins. The C-terminal end of GluR6a interacts with the PDZ proteins SAP102, SAP97, PSD-95, PICK1, and GRIP (Coussen et al., 2002; Garcia et al., 1998; Hirbec et al., 2003). GluR5b and GluR5c similarly interact with the PDZ domains of PICK1 and GRIP (Hirbec et al., 2003). It has been proposed that PICK1 interaction with KAR subunits favors KAR phosphorylation and stabilization at synapses through an interaction with GRIP. GluR6a also indirectly interacts with proteins of the cadherin/catenin complex, triggering the recruitment of KARs at cell-cell contacts (Coussen et al., 2002).

Here, we report that GluR6a and GluR6b are assembled within the same heteromeric KAR complex in vivo, even though both splice variants do not differ in their functional properties. We have questioned the biological relevance of this coassembly in terms of trafficking and function. Using a proteomic approach following affinity purification, we have identified subsets of proteins that differentially interact with these two splice variants. This provides evidence that heteromeric as-

*Correspondence: mulle@u-bordeaux2.fr

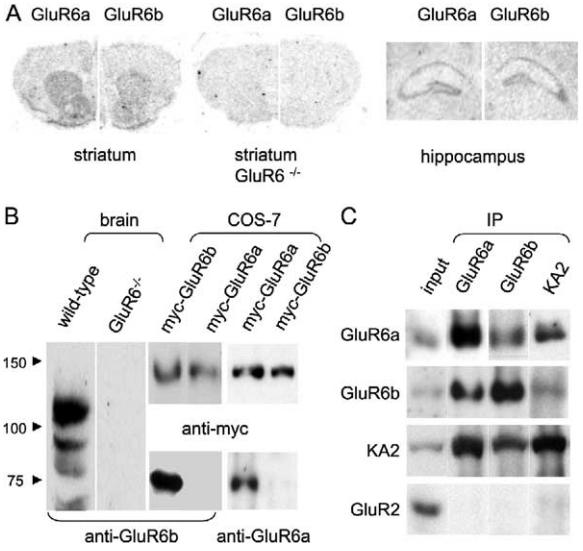

Figure 1. Interaction between GluR6a and GluR6b in Mouse Brain

(A) In situ hybridization with specific oligonucleotide probes for GluR6a or GluR6b C-terminal domains. Frontal sections at two different levels of mouse brains show strong hybridization signals in the striatum (left) and the hippocampus (right) with both oligonucleotides. No labeling appeared in sections of GluR6$^{-/-}$ mice taken at the striatal level (center).

(B) Characterization of GluR6b-specific antibody. Anti-GluR6b was probed against membrane proteins from wild-type or GluR6$^{-/-}$ mice brain. The antibody recognized a protein of 115 kDa, which was not detectable in KO mice. Additional bands of lower molecular weight labeled by the anti-GluR6b antibody likely correspond to proteolytic fragments, since they were not observed in GluR6$^{-/-}$ mice. When equivalent amounts of GluR6a and GluR6b subunits expressed in COS-7 cells were loaded on gels, as assessed by anti-myc immunoblotting, the antibody recognized specifically the GluR6b subunit. Anti-GluR6/R7 antibody is specific for the GluR6a form. (C) Coimmunoprecipitation of KAR subunits in mouse brain. Proteins solubilized from mouse brain membranes were immunoprecipitated with specific KAR antibodies (IP). Immunoprecipitated proteins were detected using corresponding antibodies. KAR subunits each coimmunoprecipitated with one another but did not immunoprecipitate the GluR2 AMPAR subunit.

sembly of two splice variants of GluR6 increases the repertoire of interacting partners for KARs and brings together proteins that contribute to the regulation of KAR function.

Results

Heteromerization of Two C-Terminal Splice Variants of GluR6

Mouse GluR6a and GluR6b (originally named GluR6-2 in mouse) differ by a stretch of 54 and 15 amino acids, respectively, at the ends of their C-terminal domains. In a previous report, we showed that the splice variants GluR6a and GluR6b were equally well detected at the mRNA level in large brain regions using RT-PCR (Jaskolski et al., 2004). To better define the respective expression patterns of the splice variants, we performed in situ mRNA localization using specific oligonucleotide primers corresponding to GluR6a and GluR6b C-terminal domains (Figure 1A). Transcripts for GluR6a and GluR6b were detected in the same neuronal populations, in the striatum or principal cells of the hippocampus (Figure 1A). No labeling was detected in GluR6$^{-/-}$ mice for both GluR6a and GluR6b probes.

We thus examined whether GluR6a and GluR6b could form heteromers in vivo. For this purpose, we produced a specific antibody directed against the GluR6b subunit that recognized a major protein of 115 kDa in a Western blot loaded with brain membranes from wild-type mice, but not from GluR6$^{-/-}$ mice (Figure 1B). The anti-GluR6b antibody labeled a band on membranes prepared from COS-7 cells transfected with GluR6b, but not from cells transfected with GluR6a (Figure 1B). Conversely, the GluR6/7 antibody, which is directed against an amino acid sequence present in GluR6a, does not recognize GluR6b in COS-7 cells (Figure 1B). The calculated molecular weight for GluR6b is 98 kDa. The 115 kDa protein detected in brain membranes could correspond to a glycosylated form of GluR6b, as already shown for transfected COS-7 cells (Jaskolski et al., 2004).

Taking advantage of GluR6a and GluR6b antibodies, we investigated whether GluR6a and GluR6b were part of the same KAR complex in mouse brain. GluR6a was immunoprecipitated by the GluR6b antibody and, conversely, GluR6b was immunoprecipitated by the GluR6/7 (GluR6a) antibody (Figure 1C). KA2 subunit also coimmunoprecipitated with GluR6a and GluR6b, but the AMPA receptor subunit GluR2 did not. These results indicate that GluR6a and GluR6b can assemble in vivo within the same KAR complex, together with KA2.

Electrophysiological Characterization of GluR6a/GluR6b Heteromers

To further confirm that GluR6a and GluR6b can coassemble within the same receptor, we used an electrophysiological assay that takes advantage of the different rectification properties of the Q/R editing isoforms of GluR6 (Bowie and Mayer, 1995). We first expressed the nonedited variants (Q forms) of GluR6a and GluR6b individually in HEK293 cells. The amplitude of inward currents evoked by fast application of glutamate (1 mM) (Figure 2A) was about 10-fold larger for GluR6a(Q) than for GluR6b(Q) (Figure 2B) (GluR6a: 3,914 ± 912 pA, n = 15; GluR6b: 306 ± 69 pA, n = 15), in agreement with differences in plasma membane targeting of the two splice variants (Jaskolski et al., 2004). The evoked currents desensitized rapidly and almost completely for both splice variants, as previously described for GluR6a(Q) receptors (Bowie and Mayer, 1995; Traynelis and Wahl, 1997). Single exponential fits to the desensitizing phase had time constants of 9.4 ± 0.5 ms (n = 15) for GluR6a(Q) and 10.2 ± 0.8 ms for GluR6b(Q), which were not significantly different (p = 0.4).

The Q to R substitution in GluR6 homomers decreases unitary conductance of the channels, reduces calcium permeability, and transforms the rectification properties of these receptors from inwardly rectifying to linear or slightly outwardly rectifying (Bettler and Mulle, 1995; Lerma, 2003). Indeed, the amplitudes of currents evoked at −40 mV in cells expressing GluR6a(R) or GluR6b(R) were much smaller than those for their counterparts with the Q form (Figure 2B), with GluR6b(R) be-

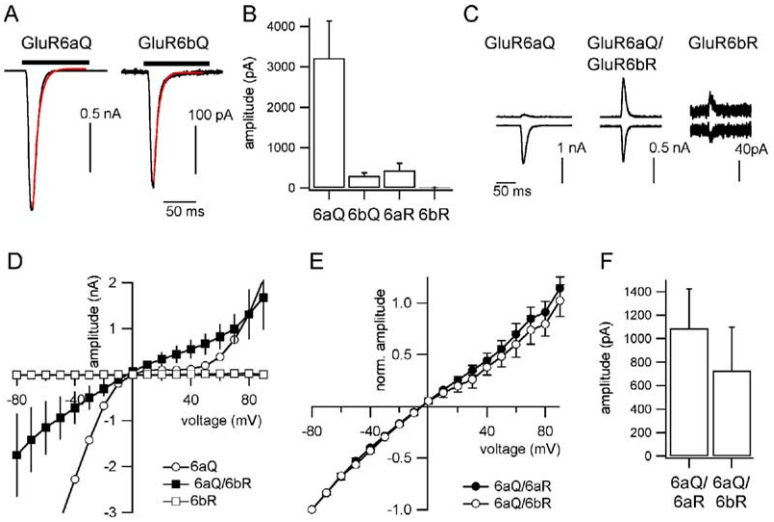

Figure 2. GluR6a and GluR6b Form Functional Receptors and Heteromerize

(A) Examples of currents evoked by 1 mM glutamate in cells transfected with unedited (Q form) GluR6a (left) or GluR6b (right). The red lines represent single exponential fits of the decay, with time constants of 8.5 and 7.6 ms, respectively. (B) Amplitudes of currents evoked by 1 mM glutamate at –40 mV, in cells transfected with various GluR6 splice and editing variants (n = 5 to 15 cells for each condition). (C) Currents evoked in cells transfected with the constructs shown above, at –40 mV and +40 mV. (D) IV curves for glutamate-evoked currents in cells expressing GluR6a(Q), GluR6b(R), or expressing both subunits. (E and F) Currents evoked in cells expressing GluR6a(Q) and either GluR6a(R) (n = 6 cells) or GluR6b(R) (n = 5 cells) have similar IV curves (E) and amplitudes (F). In (E), current amplitudes for each cell were normalized to the value at –80 mV. Error bars represent ±SEM.

ing barely detectable (Figure 2C). In addition, the Q/R substitution led to an outwardly rectifying I/V curve (data not shown). If GluR6a and GluR6b coassemble within the same receptor, coexpressing GluR6a(Q) and GluR6b(R) should lead to the expression of receptors that have a linear I/V curve, which is a strategy that has been used to monitor the heteromerization of other GluR subunits (Ayalon and Stern-Bach, 2001; Bortolotto et al., 1999; Cui and Mayer, 1999; Paternain et al., 2000). Coexpression of both splice variants led to much larger currents at positive potentials than in cells expressing either GluR6a(Q) or GluR6b(R) alone as homomers (Figures 2C and 2D). These currents cannot be attributed to the sum of homomeric GluR6a(Q)- and GluR6b(R)-mediated currents due to the very low amplitude of homomeric GluR6b(R) currents. These data thus indicated that both splice variants were coassembled.

In these experiments, we also confirmed that GluR6a promoted the surface expression of GluR6b, a splice variant which is largely retained in the endoplasmic reticulum (ER) when expressed as a homomeric protein (Jaskolski et al., 2004). We compared cells expressing GluR6a(Q)/GluR6a(R) and cells expressing GluR6a(Q)/GluR6b(R). The I/V curves (Figure 2E) and amplitudes (Figure 2F) of the evoked currents were almost identical, showing that the two splice variants coassembled and were targeted to the plasma membrane equally as well as receptors composed of only GluR6a.

Consequences of the Coassembly of GluR6a and GluR6b

We examined in further detail the consequences of the coassembly of GluR6a and GluR6b in regard to the trafficking of KARs to the plasma membrane. For this purpose, we transfected cell lines and neurons in culture with epitope-tagged GluR6 splice variants. GluR6a (or myc-GluR6a) and GluR6b (or myc-GluR6b) were cotransfected in COS-7 cells. 98% ± 1% of GluR6b coimmunoprecipitated with myc-GluR6a, (n = 3 experiments) and 78% ± 11% of GluR6a coimmunoprecipitated with myc-GluR6b (n = 3) (Figure 3A). We used a biotinylation assay to quantify the amount of KAR proteins expressed at the cell surface. The biotinylated fraction of myc-GluR6a represented 91% ± 8% of the total myc-GluR6a when expressed alone in COS-7 cells, an amount which did not vary when coexpressed with GluR6b (Figure 3B) (92% ± 8%, n = 4). Whereas a large proportion of myc-GluR6b protein remained in intracellular compartments (biotinylated fraction, 53% ± 11%, n = 5) when expressed alone, the large majority of GluR6b (83% ± 7%, n = 5) was detected in the extracellular fraction when myc-GluR6b was coexpressed with GluR6a. To examine the distribution of the two splice variants on the plasma membrane of COS-7 cells by immunocytochemistry (Figure 3C), we transfected the two splice variants fused to two different extracellular epitopes (GPF-GluR6a and myc-GluR6b). When expressed separately, both GFP-GluR6a and myc-GluR6b formed aggregates at the plasma membrane, but only GFP-GluR6a was concentrated at intercellular junctions, consistent with the specific interaction of GluR6a with cadherin/catenin proteins (Coussen et al., 2002). In cells cotransfected with GluR6a and GluR6b, the extracellular localization of myc-GluR6b matched almost exactly that of GFP-GluR6a, and was consequently concentrated at intercellular junctions (Figure 3C). In cultured hippocampal neurons derived from GluR5$^{-/-}$ × GluR6$^{-/-}$ mice, myc-GluR6b expressed at the surface of the dendritic membrane was similarly colocalized entirely with GPF-GluR6a (Figure 3D). Thus, when GluR6a and GluR6b are coexpressed in heterologous cells or in cultured neurons, GluR6b readily coassembles with GluR6a, positively regulating the trafficking of GluR6b to the plasma membrane and to intercellular junctions.

Identification of Proteins Interacting with GluR6a

Since both GluR6a and GluR6b were expressed in the same neuronal populations and coassembled in native receptors, we hypothesized that heteromerization of GluR6a and GluR6b could extend the repertoire of cyto-

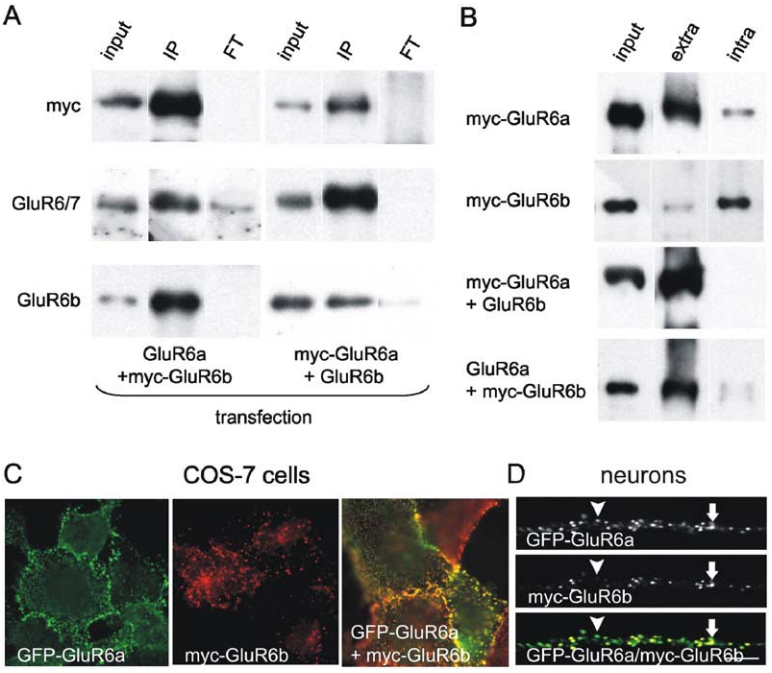

Figure 3. Role of GluR6a/GluR6b Heteromerization on the Membrane Localization of KARs

(A) Coimmunoprecipitation of GluR6a and GluR6b in COS-7 cells. COS-7 cells were cotransfected either with GluR6a/myc-GluR6b or with GluR6b/myc-GluR6a. After 24 hr of expression, immunoprecipitation was performed, using an anti-myc antibody and Western blots analyzed with anti-myc, anti-GluR6a, and anti-GluR6b antibodies. Both myc-tagged subunits were immunoprecipitated (100%) and their counterpart coimmunoprecipitated with the tagged subunit.

(B) Surface localization of the receptor subunits. Biotinylation assays were performed on COS-7 cells expressing the different receptors: biotin binds to extracellular proteins, "input" corresponds to 5% of total proteins, "extra," to the biotinylated extracellular protein, and "intra," to nonbiotinylated intracellular proteins. Heteromerization of GluR6b with GluR6a promoted the extracellular localization of GluR6b without affecting GluR6a.

(C) Extracellular labeling of GFP-GluR6a (green) and myc-GluR6b (red) expressed alone or in combination, in COS-7 cells. Coexpression of GluR6a and GluR6b promoted cell-surface expression of GluR6b. (D) Extracellular labeling of myc-GluR6b and GFP-GluR6a expressed in combination, in hippocampal neurons in culture. Arrowhead shows expression of GluR6a in the absence of GluR6b. When expressed at the cell surface, GluR6b colocalized with GluR6a (arrow). Scale bar, 10 μm.

solic proteins associated with GluR6-containing KARs and thus might serve to bring into close proximity proteins that are functionally connected. To get a global overview of proteins interacting with the receptor C terminus of both splice variants, we used a proteomic approach that combined either pull-down or coimmunoprecipitation experiments, 2-D electrophoresis, and identification of proteins by MALDI-TOF mass spectrometry. To identify the proteins that specifically interact with the GluR6a C terminus, we performed differential analyses of: (1) proteins that were recruited by the entire GluR6a C terminus fused to GST, but not by GST alone (Figures 4A and 4B) and (2) proteins that were immunoprecipitated by the anti-myc antibody from membrane extracts of transgenic mice expressing myc-GluR6a (which represents 25% of the wild-type GluR6 protein) (Coussen et al., 2002) (Figure 4C) or of wild-type animals (data not shown). Fifteen spots or trains of spots were present in 2D gels of both GST pull-down experiments with the C-terminal domain of GluR6a (Figure 4A) and immunoprecipitation with a myc antibody from transgenic mouse brains (Figure 4C), but were not detected when GST alone was used as a bait (Figure 4B). Among the 15 spots, we were able to identify six different proteins from their peptide mass fingerprint determined by MALDI-TOF mass spectrometry (listed in Table 1). These proteins are spectrin (spot 1), Contactin chain 1 or F3-contactin (2), dynamin-1 (3), dynamitin (4), 14-3-3 γ (5), and calmodulin (6). All these proteins were specifically immunoprecipitated with the anti-myc antibody from brain extracts of mice expressing myc-GluR6a, indicating that they interact with native GluR6a in vivo (Figures 4C and 4D).

Identification of Proteins Interacting with GluR6b

No binding partner of GluR6b has yet been identified. Proteins that specifically interact with the GluR6b C-terminal domain were isolated by peptide affinity chromatography, using a synthetic peptide encompassing the last 15 C-terminal amino acids of GluR6b as bait and separated onto 2D gels (Figure 5). Eight spots that were apparent in the gels obtained with the GluR6b C-terminal peptide (Figure 5A) were undetectable in the gels obtained by incubating brain extracts with beads not coupled to the peptide (Figure 5B). Seven spots were unambiguously identified by MALDI-TOF mass spectrometry (Table 1). These spots corresponded to calmodulin (spot 6), protein phosphatase 2B (both the catalytic β and the regulatory α subunits, 7 and 11), N-ethylmaleimide-sensitive fusion protein attachment protein γ (NSF, 8), visinin-like protein 1 or VILIP-1 (9), neurocalcin delta or VILIP-3 (10), and profilin II (12). The identity of proteins that display specific interaction with the GluR6b C terminus in pull-down experiments was confirmed by immunoblotting with specific antibodies (Figure 5C). However, interactions detected in peptide pull-down experiments could be due to nonspecific interactions between the GluR6b peptide and the cytosolic proteins, since the amount of peptide is much higher than in physiological conditions. We thus performed coimmunoprecipitation experiments from mouse brain to determine whether these proteins interact with native KARs. The GluR6b antibody was not used in these experiments because it recognizes a sequence corresponding to the GluR6b C-terminal domain, likely precluding the detection of proteins that interact with the same domain of the GluR6b sequence. We there-

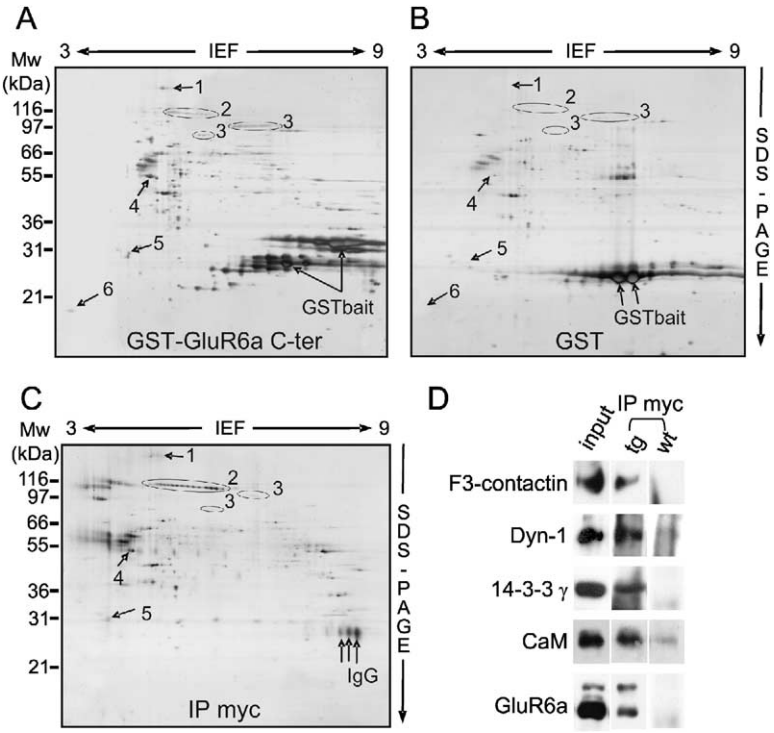

Figure 4. Identification of Proteins Interacting with GluR6a C Terminus

(A and B) GST pull-down using GluR6a C terminus as bait. Cytosolic fraction from mouse brain (6 mg protein) was incubated with GST fused to the GluR6a C terminus (A) or GST alone (B) immobilized on glutathione-Sepharose beads. Proteins retained by affinity were separated by two-dimensional electrophoresis and stained with silver. (C) Coimmunoprecipitation of proteins with myc-GluR6a. Triton X-100 extract proteins (4 mg protein) from transgenic mice expressing myc-GluR6a were immunoprecipitated with an anti-myc antibody. Immunoprecipitated proteins were separated onto 2D gels. Typical gels, representative of three independent experiments, are illustrated. Arrows indicate the position of spots identified by MALDI-TOF mass spectrometry (see Table 1) that are not detectable in gels from pull-down experiments performed with GST alone (B) or immunoprecipitation performed from wild-type mouse (data not shown). (D) Western blot analysis of proteins that coimmunoprecipitate with myc-GluR6a. "Input" represents 5% of the total amount of protein used in immunoprecipitation. tg, transgenic myc-GluR6a mice.

fore used myc-GluR6a transgenic mice (Coussen et al., 2002). We first verified that in these mice, native GluR6b was coimmunoprecipitated with myc-GluR6a, and vice versa (Figure 5D). Since myc-GluR6a coassembled with GluR6b, proteins interacting with GluR6b may coimmunoprecipitate with myc-GluR6a. Consistent with this hypothesis, proteins interacting with GluR6b in our in vitro binding assay were immunoprecipitated with the anti-myc antibody (Figure 5C). This finding confirms that the proteins identified do interact with GluR6b in vivo, and also brings further support to the finding that GluR6a and GluR6b are part of the same heteromeric receptor in vivo.

Strikingly, several GluR6b binding partners that we have identified are known to function in a Ca^{2+}-dependent manner. This is the case for calmodulin, calcineurin, and the VILIP proteins. We thus checked whether interactions between the GluR6b C-terminal peptide

Table 1. Proteomic Analysis of Proteins Interacting with the C Terminus of the KAR Splice Variants GluR6a and GluR6b

Position in Gels (Figures 4 and 5)	Protein	Accession Number*	MALDI-TOF MS		GluR6a	GluR6b
			Peptides	Coverage (%)		
1	Spectrin	O88663	32	20.6	+	–
2	Contactin chain 1	P12960	18	31.9	+	–
3	Dynamin-1	P39053	18	21.4	+	–
4	Dynamitin	Q99KJ8	12	38.6	+	–
5	14-3-3 protein γ	P35214	5	26.0	+	–
6	Calmodulin	P02593	10	70.3	+	+
7	Protein phosphatase 2B catalytic subunit, β isoform	P48453	19	36.9	–	+
8	N-ethylmaleimide sensitive fusion protein attachment protein γ	Q8C1T5	7	26.0	–	+
9	Visinin-like protein 1 (VILIP-1)	P28677	9	48.4	–	+
10	Neurocalcin delta (VILIP-3)	Q91X97	9	40.1	–	+
11	Protein phosphatase 2B regulatory subunit 1, α isoform	Q63810	4	29.6	–	+
12	Profilin II	Q9JJV2	5	36.7	–	+

*The SWISS-PROT and TrEMBL accession numbers are listed.

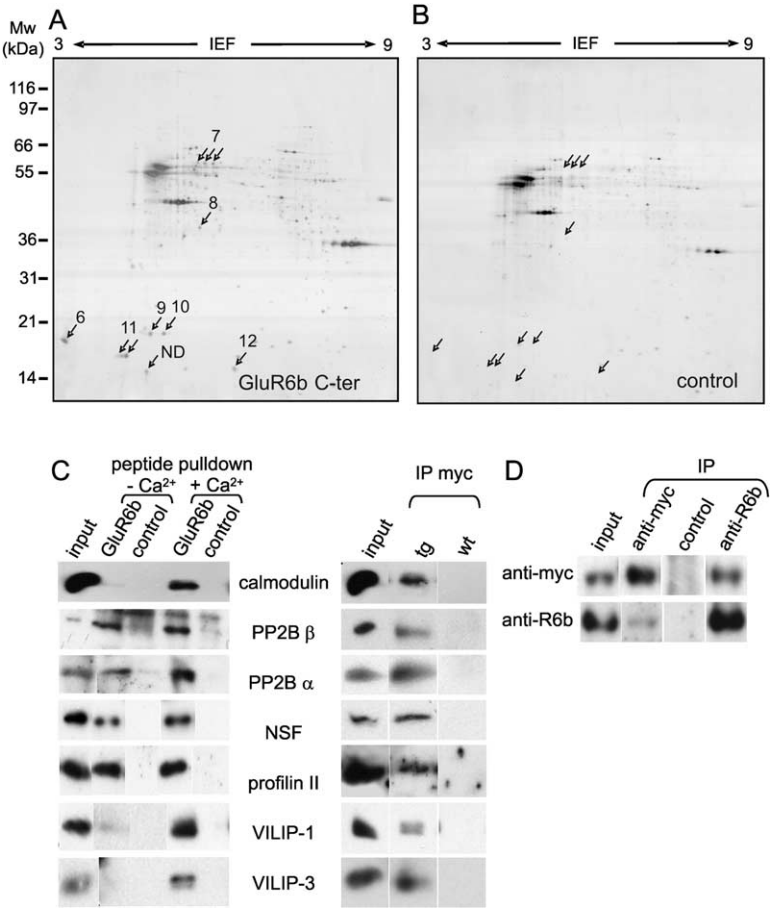

Figure 5. Identification of Proteins Interacting with the GluR6b C Terminus

(A and B) Cytosolic fraction from mouse brain (4 mg protein) was incubated with a synthetic peptide encompassing the 15 C-terminal residues of GluR6b and immobilized on activated Sepharose beads (A) or with the Sepharose beads alone ([B], control). 2D gels representative of three experiments performed independently are illustrated. Arrows indicate the position of spots that were specifically recruited by the GluR6b C-terminal peptide. ND, not determined by MALDI-TOF mass spectrometry. (C) Western blot analysis of proteins recruited by the GluR6b C-terminal peptide and identified by MALDI-TOF mass spectrometry. Left panel: peptide-affinity chromatography using the GluR6b C-terminal peptide as bait was performed in the absence (5 mM EDTA) or presence of 5 mM Ca^{2+}. Input represents 5% of the total amount of protein used in pull-down experiments. Right panel: immunoprecipitation of proteins identified as binding partners of GluR6b with an anti-myc antibody in detergent-solubilized extracts from transgenic myc-GluR6a mice. Proteins in immunoprecipitates were detected by immunoblotting. Input represents 5% of the total amount of protein used in immunoprecipitation. (D) Coimmunoprecipitation of GluR6b and myc-GluR6a in αCaMKII-myc GluR6a transgenic mice. Immunoprecipitation was performed using either anti-myc or anti GluR6b antibodies. Western blots were then probed with the corresponding antibodies. Control lane, no primary antibody. Tg, transgenic myc-GluR6a mice.

and its partners were dependent on Ca^{2+}. We incubated cytosolic fractions from mouse brain with GluR6b C-terminal peptide either in a buffer with Ca^{2+} (5 mM) or with EDTA (5 mM) (Figure 5C). Calmodulin bound to the GluR6b C-terminal peptide only in the presence of Ca^{2+} (n = 4). Binding of VILIP proteins to the GluR6b C terminus was also dramatically reduced in the absence of Ca^{2+}. In contrast, the binding of calcineurin (both the catalytic and regulatory subunits) was less sensitive to Ca^{2+} than that of calmodulin or the VILIP family proteins. Finally, interactions between profilin II or NSF and the GluR6b C-terminal peptide were not dependent on the presence of Ca^{2+}.

Control of the Calcium-Dependent Depression of Neuronal KARs by Calcineurin Binding to GluR6b

Since GluR6a and GluR6b interact with distinct subsets of protein partners, we hypothesized that the binding of protein partners separately to the two GluR6 splice variants could induce a crossregulation of the GluR6 heteromer. We thus evaluated the importance of the heteromerization of GluR6a and GluR6b for native KAR function. We focused on the role of calcineurin, because its role in the physiology of native and recombinant KARs has been well documented. Phosphorylation of recombinant GluR6a by PKA increases receptor function (Wang et al., 1993) by increasing its opening probability (Traynelis and Wahl, 1997), while calcineurin has the opposite effect (Traynelis and Wahl, 1997). Moreover, in hippocampal neurons in culture, the rise in intracellular calcium concentration caused by activation of NMDA receptors or voltage-gated calcium channels causes a transient depression of KAR-mediated currents (Ghetti and Heinemann, 2000). This depression is maximal within 1 s after Ca^{2+} entry and appears to require calcineurin; the recovery from depression is complete within 10 s and requires the phosphorylation of KARs by CamKII (Ghetti and Heinemann, 2000). Therefore, we hypothesized that such a fast depression would require direct binding of calcineurin to the receptor through the GluR6b subunit. In mouse hippocampal neurons in culture, KAR currents activated by kainate (300 μM) were transiently depressed after prior application of NMDA for 3 s (Figure 6A). The depression lasted less than 10 s and was most prominent at the earliest interval tested, i.e., 2 s (63% ± 5% of control current, n = 10) (Figure 6C). This depression was dependent on a rise in intracellular Ca^{2+}, since no depression was observed when 10 mM BAPTA was included in the recording solution (90% ± 7% of control current 2 s after NMDA application, n = 3). Then, using the recording patch pipette, we dialyzed the C-terminal GluR6b peptide (15 amino acids, pepR6b) to compete for proteins interacting with this subunit. In pull-down experiments,

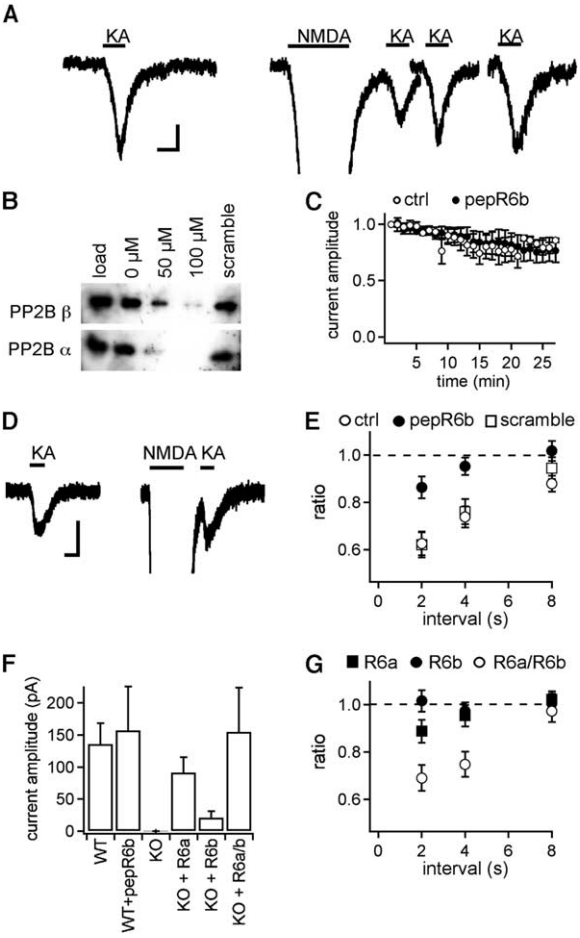

Figure 6. Disruption of Calcineurin Binding to the GluR6b Subunit Suppresses Ca^{2+}-Induced Depression of Native KARs

(A) Currents evoked by 300 μM kainate (KA) alone (left) or with previous applications of NMDA (200 μM, 3 s) at 2, 4, and 8 s intervals (right). Scale bar, 100 pA, 1 s. The cell was recorded in control intracellular solution. (B) Competition assay by R6b peptide in GST-pull-down experiments. Binding of calcineurin was inhibited by incubation of 100 μM of pepR6b peptide. Incubation with the scramble peptide did not have any effect. (C), Intracellular dialysis of pepR6b peptide did not affect KA-evoked currents (n = 4 for each condition). (D) In the presence of pepR6b, application of NMDA did not depress the KA-evoked current. Experimental conditions as in (A). (E) Summary of experiments as in (A) and (D). Plot of the ratio of KAR current with or without NMDA preapplication, at various intervals. White circles, control solution (n = 10); black circles, with R6b peptide (n = 5); white squares, with scrambled peptide (n = 6). (F) KA-evoked current amplitudes in different cells: wild-type cells in control solution (WT, n = 15) and solution containing pepR6b (n = 9); cells from GluR5,$6^{-/-}$ mice, not transfected (KO, n = 5) or transfected with GluR6a (n = 5), GluR6b (n = 6), or both (n = 6). (G) Plot as in (E) for cells from KO mice transfected with GluR6a (n = 4), GluR6b (n = 3), or both (n = 6). Error bars represent ±SEM.

binding of calcineurin to GluR6b was inhibited in a dose-dependent manner by preincubation with the pepR6b peptide (Figure 6B). Dialysis of this peptide did not affect the average amplitude nor the run-down of KAR currents (Figures 6C and 6F), suggesting that binding of proteins to the GluR6b subunit was not required for plasma membrane targeting on the timescale of minutes. However, after more than 5 min of recording to allow for dialysis of the peptide, the depression of KAR current caused by NMDA was significantly reduced compared to the control condition with no peptide (Figures 6D and 6E) (depression to 86% ± 5% of control, 2 s after NMDA application, n = 5, $p < 0.005$). To test for a nonspecific effect of pepR6b, we dialysed a scrambled peptide (see Experimental Procedures); the depression was identical to the one observed without peptide (Figure 6C, 62% ± 5% of control after 2 s, n = 6). Since the depression was reported to be dependent on dephosphorylation of KARs by calcineurin, our data suggest that binding of calcineurin to GluR6b contributes to the regulation of native KARs following Ca^{2+} entry.

Thus, coassembly of GluR6a and GluR6b subunits is likely necessary for the expression of KAR regulation by intracellular calcium. To test this hypothesis, we transfected KAR subunits in cultured neurons derived from GluR5$^{-/-}$ × GluR6$^{-/-}$ mice. Untransfected cells did not show any current in response to kainate with the antagonist cocktail (Figure 6F, n = 5). Interestingly, knock-out neurons transfected with the GluR6a subunit displayed KAR-mediated currents with amplitudes similar to those in untransfected wild-type neurons (Figure 6F), indicating that the transfection protocol did not lead to gross overexpression of the exogenous receptors. Cells transfected with GluR6b alone displayed significantly smaller KAR-mediated currents (Figure 6F, $p < 0.05$ compared with wild-type), consistent with reduced plasma membrane targeting of this subunit when expressed alone (Jaskolski et al., 2004). KARs made with only one type of GluR6 subunit were not affected by preapplication of NMDA, and only when the two splice variants were coexpressed, did NMDA significantly depress the receptors (Figure 6G), showing the crucial importance of the heteromerization of two splice variants for this effect.

Discussion

In the present study, we demonstrate that two splice variants of the same KAR subunit, GluR6a and GluR6b, coassemble to form heteromers in heterologous cell systems and in the brain. We provide evidence that such heteromerization in recombinant and native KARs is crucial for crossregulation between the C-terminal domains of the two splice variants through differential association with cytosolic proteins. These data highlight a feature of alternative splicing that allows corecruitment of sets of cytosolic interacting proteins within a glutamate receptor molecular complex.

The C-terminal domain of ionotropic glutamate receptors contains critical determinants for receptor trafficking and is subject to alternative splicing in most glutamate receptors. Complex interactions of C-terminal domains with proteins that include PDZ proteins are important for the regulated trafficking of AMPA and NMDA receptors, especially during synaptic plasticity. By in situ hybridization analysis, we indicate that GluR6a and GluR6b, two splice variants that differ in their C-terminal domain, are expressed in the same neuronal pop-

ulations. This raises the question of the biological significance of the coexpression, in a single neuron, of two splice variants that do not appear to differ in their functional properties. In the present study, we provide strong evidence that GluR6a and GluR6b coassemble as heteromers in native KARs (likely together with the KA2 subunit). The essential NR1 subunit of NMDA receptors also exists in several isoforms generated by alternative splicing (Zukin and Bennett, 1995). Whereas splicing of an exon in the N-terminal domain regulates the pharmacological properties of NMDARs, alternative splicing of C-terminal exons influences protein interactions and intracellular trafficking (Wenthold et al., 2003). Interestingly, activity-dependent targeting of NMDA receptors to synaptic sites is controlled by regulated mRNA splicing of NR1 in the C-terminal domain (Mu et al., 2003). Despite biochemical evidence that NR1 splice variants with different C-terminal domains can compose native NMDARs (Chazot and Stephenson, 1997; also see Sheng et al., 1994), the biological implication for this coassembly has not yet been directly addressed.

The presence of two GluR6 subunits with distinct C-terminal domains within the same KAR complex likely extends the possibilities of interaction with cytosolic proteins. Accordingly, we have identified two distinct subsets of protein partners that differentially interact with one or the other splice variant. These include six proteins that bind to the C-terminal domain of GluR6a. These proteins were identified in both GST pull-down extracts and immunoprecipitates from transgenic mice expressing myc-GluR6a receptors in forebrain neurons (Coussen et al., 2002). Surprisingly, we did not detect a set of PDZ proteins such as PSD-95, SAP102, SAP97, CASK, GRIP, PICK1, and syntenin, which have been shown to interact with the GluR6a C terminus in previous studies (Coussen et al., 2002; Garcia et al., 1998; Hirbec et al., 2003). This is not due to the inability of our approach to detect PDZ-based interactions, because we have already identified PDZ proteins as binding partners of the serotonin 5-HT_{2A} and 5-HT_{2C} receptors, which express a canonical class I PDZ binding motif (SXV), using a similar proteomic screen (Becamel et al., 2004). One reason for nondetection of these proteins could be that the PDZ binding motif of GluR6a (TMA) is less efficient than more classical class I PDZ recognition motifs (S/TXV/I/L) for binding to PDZ proteins. Consistent with this hypothesis, the mutation of the valine at the position 0 to alanine in such PDZ ligands drastically reduces binding to PDZ partners (Becamel et al., 2004; Nourry et al., 2003). In parallel, we have identified, using a peptide pull-down assay, seven proteins interacting with the C-terminal domain of GluR6b. To ascertain that these proteins interacted with GluR6b, we used myc-GluR6a transgenic mice in which GluR6b coassembles with myc-GluR6a. Using an anti-myc antibody we immunoprecipitated myc-GluR6a/GluR6b receptors and confirmed by Western blotting the interaction of all seven proteins identified as GluR6b binding partners.

The proteins interacting with GluR6a/GluR6b comprise proteins possibly involved in the assembly and trafficking of membrane proteins, such as 14-3-3 γ, dynamin-1, NSF, and dynamitin. 14-3-3 proteins perform a large variety of physiological functions through mechanisms that include regulation of enzyme activity, stimulation of protein-protein interactions, and control of the subcellular localization of a binding partner (Berg et al., 2003). In particular, 14-3-3 proteins play an essential role in controlling the function and localization of ion channels. For instance, in the K^+ channel subunit Kir6.2, 14-3-3 proteins interact with a cytoplasmic ER-retention motif and promote forward trafficking to the plasma membrane (Yuan et al., 2003). In addition, surface expression of KCNK3 K^+ channels is achieved by the phosphorylation-dependent binding of 14-3-3 β and release from COPI-mediated ER retention (O'Kelly et al., 2002). Similarly, binding of 14-3-3γ to the C-terminal domain of GluR6a might be instrumental for the efficient forward trafficking of homomeric and heteromeric receptors containing this subunit (Jaskolski et al., 2004; Yan et al., 2004). Dynamins are known to be essential for receptor-mediated endocytosis, although the role of these GTPases probably extends beyond endocytosis (Sever, 2002). Endocytosis of AMPA and NMDA receptors is blocked by overexpression of a dominant form of dynamin (Carroll et al., 1999; Man et al., 2000; Nong et al., 2003; Wang and Linden, 2000), but the subtype of dynamin involved in this process has not been identified. Here we show that GluR6a interacts with dynamin-1. Dynamin-1 is concentrated in the presynaptic compartment (Gray et al., 2003) and is best known for its participation in synaptic vesicle recycling, arguing against the possibility that it plays a role in the endocytosis of glutamate receptors in postsynaptic neuronal domains. However, the presence of GluR6a in presynaptic terminals (Jaskolski et al., 2004) would be consistent with an interaction with dynamin-1. It will be necessary to evaluate whether this interaction is related to the presynaptic function of KARs in regulating neurotransmitter release (Huettner, 2003; Jaskolski et al., 2005; Lerma, 2003), whether dynamin-1 is involved in the endocytosis of presynaptic KARs, or whether interaction with dynamin-1 is unrelated to endocytosis (Sever, 2002). Interaction of GluR6b with NSF, a protein involved in membrane fusion, is reminiscent of its role in the expression of GluR2-containing AMPA receptors at synapses and its role in long-term depression (Nishimune et al., 1998; Song et al., 1998). Further studies have elucidated a role for NSF in stabilizing AMPA receptors (Braithwaite et al., 2002) or in promoting the recycling of internalized GluR2-containing AMPA receptors (Lee et al., 2004). Dynamitin, which binds to GluR6a, is part of the dynactin complex, a multisubunit protein complex required for the activity of the molecular motor dynein (Schroer, 2004), with a role in retrograde as well as anterograde axonal transport (Vallee et al., 2004). Interaction of GluR6a to dynamitin might thus be involved in the trafficking of KARs along the axon. In addition to the proteins identified in the present study, a number of PDZ domain binding proteins are thought to be implicated in the regulated trafficking and stabilization of KARs in specific neuronal domains, such as PSD-95, GRIP, PICK1, and CASK/Lin proteins.

Two proteins interacting with GluR6a/GluR6b are involved in the organization of the cytoskeleton. First, spectrin localizes to the postsynaptic density and could serve to link KARs to the actin cytoskeleton, as in the

case of NMDA receptors (Wechsler and Teichberg, 1998). Second, profilin II, a small actin binding protein implicated in regulating actin polymerization (Witke et al., 1998), is targeted to dendritic spine heads following robust synaptic activation and might play a role in stabilizing dendritic spine morphology (Ackermann and Matus, 2003). Profilin II, by controlling actin stability, is also involved in the regulation of neuritogenesis by RhoA activity (Da Silva et al., 2003). Along these lines, regulation of the motility of hippocampal mossy fiber filopodia by KARs (Tashiro et al., 2003) might rely on the interaction of GluR6a/GluR6b with profilin II.

Finally, a third group of proteins interacting with the C-terminal domains of GluR6b comprises proteins involved in the Ca^{2+} regulation of ion channels and receptors: calcineurin (PP2Bα and PP2Bβ subunits), calmodulin (which also binds to GluR6a), VILIP-1, and VILIP-3. The binding of these proteins to GluR6b depends on Ca^{2+}. VILIP-1 and VILIP-3 belong to a large family of Ca^{2+} sensor proteins involved in a variety of Ca^{2+}-dependent signal transduction cascades, e.g., by coupling intracellular Ca^{2+} to the modulation of different types of voltage-gated ion channels (Burgoyne and Weiss, 2001). The Ca^{2+}-dependent membrane association, the so-called Ca^{2+}-myristoyl switch that localizes VILIP proteins to distinct cellular signaling compartments may be a critical mechanism for the coordinated regulation of signaling cascades (Spilker and Braunewell, 2003). VILIP-1 modulates the surface expression and agonist sensitivity of the $\alpha4\beta2$ nicotinic acetylcholine receptor in response to changes in the intracellular Ca^{2+} concentration (Lin et al., 2002). There is no report of a similar effect on glutamate receptors. In contrast, the Ca^{2+} binding protein calmodulin has a well-established role in regulating the functional properties of NMDA receptors by a direct interaction with the NR1 subunit (Ehlers et al., 1996). It is widely accepted that particular patterns of synaptic activity induce a rise of intracellular Ca^{2+} concentration, which, in turn, activates kinases and phosphatases capable of modifying glutamate receptor function. Calcineurin is the predominant phosphatase in neurons that is activated by Ca^{2+} and calmodulin (Winder and Sweatt, 2001).

It is thus important to clarify how Ca^{2+}/calmodulin-dependent phophatases and Ca^{2+}/calmodulin-dependent kinases regulate the function of KARs in vivo (Ghetti and Heinemann, 2000). PKA activation enhances GluR6 function when expressed in HEK cells (Wang et al., 1993) by increasing open channel probability, whereas calcineurin decreases open channel probability (Traynelis and Wahl, 1997). In response to activation of NMDA receptors, the amplitude of KARs recorded in cultured hippocampal neurons decreases, due to the activation of calcineurin, which likely dephosphorylates KARs (Ghetti and Heinemann, 2000). Because the recovery from depression is inhibited by blockers of Ca^{2+}/calmodulin-dependent kinase, but is insensitive to blockers of PKC or PKA, CamKII activity was thought to be primarily responsible for the phosphorylation of native KARs. We took advantage of this dual regulation by calmodulin and calcineurin to provide an example in which heteromerization of GluR6 splice variants and their interaction with intracellular proteins are essential for the fine regulation of native KARs. We found that the inhibition of KAR currents by prior activation of NMDARs was largely inhibited by infusion of the neuron with a peptide corresponding to the C-terminal domain of GluR6b that binds calcineurin, and this inhibition critically depended on the presence of both GluR6a and GluR6b in the heteromeric receptor complex. Our data provide an example of cross-interaction between the C-terminal domains of GluR6a and GluR6b where GluR6b is necessary to bind an accessory protein, most likely calcineurin, and GluR6a is the likely substrate for phosphorylation/dephosphorylation that affects channel function.

In conclusion, we show that two splice variants of GluR6, a key subunit involved in the pre- and postsynaptic functions of KARs (Contractor et al., 2001; Mulle et al., 1998), coassemble in native heteromeric receptors. Coassembly of two splice variants with otherwise identical functional properties, opens the possibility for cross-regulation due to the binding of distinct subsets of proteins to the distinct C-terminal domains of the two splice variants. In this perspective, interaction of protein partners to the C-terminal domains of GluR6a and GluR6b brings together in close physical proximity functionally coupled proteins such as calmodulin and calcineurin; PDZ-domain proteins and NSF; and profilin and dynamin. These results open the way for studying multiple paired interactions and elucidating their role in the regulation of physiological and pathological functions of KARs.

Experimental Procedures

cDNA Constructs

GFP and myc cDNAs were introduced after the signal sequence in the wild-type GluR6a and GluR6b cDNAs, as previously described (Coussen et al., 2002). Site-directed mutagenesis was performed using the QuickChange XL kit (Stratagene). cDNAs were sequenced and expressed in HEK cells to check for their physiological properties.

GluR6b Antibody Production and Purification

Peptide corresponding to the last 15 amino acids of GluR6b (H_2N-KESSIWLVPPYHPDTVC-$CONH_2$) was synthesized by Eurogentec (Seraing), coupled to a carrier, injected into two rabbits, and then boosted four times during a period of three months. Antibodies were purified by peptide affinity.

In Situ Hybridization

Specific probes for GluR6a (5′-TGCCATGGTTTCTTTACCTGGCAACCTTCTGTCGTTAAATGTGTG-3′) and GluR6b (5′-AACAGTGTCTGGATGGTATGGTGGCACTAACCAAATAGAAGATTC-3′) were labeled by tailing the primers 3′ end with ^{35}S-ATP. In situ hybridization was performed as in Bernard et al. (1992).

Immunocytochemistry

COS-7 cells were transfected with cDNAs using a Fugene kit (Roche Diagnostics). Primary cultures of hippocampal neurons were obtained from 1-day-old pups of GluR5$^{-/-}$ × GluR6$^{-/-}$ mutant mice, as previously described (Jaskolski et al., 2004). They were transfected with Lipofectamine 2000 (Invitrogen). Cells were incubated 30 min at 20°C with monoclonal anti-GFP or polyclonal anti-myc antibodies (1:500 dilution) in culture media and immediately fixed with paraformaldehyde. The secondary fluorescent antibodies (anti-mouse antibody, Alexa-488, and anti-rabbit antibody, Alexa-568) were incubated for 30 min at 20°C. Coverslips were then

mounted with Prolong Antifade Kit (Molecular Probes). Pictures were taken with an Axioplan Zeiss microscope

Electrophysiology

Electrophysiological Recordings of Glutamate-Evoked Currents in HEK293 Cells

Cells were transfected using the Fugene kit with untagged GluR6 subunits and GFP at a ratio of 2:1 or 1:1:1 when one or two subunits were cotransfected with GFP. For recordings, 1 day after transfection, cells were placed in HEPES-buffered solution (HBS) containing 145 mM NaCl, 2 mM KCl, 2 mM $MgCl_2$, 2 mM $CaCl_2$, 10 mM glucose, 10 mM HEPES, adjusted to 320 mOsm and pH 7.4 with NaOH, at room temperature. Cells were observed with fluorescent illumination, and isolated, brightly fluorescent cells were chosen. Recording pipettes were filled with a solution containing 122 mM CsCl, 2 mM NaCl, 2 mM $MgCl_2$, 10 mM EGTA, 10 mM HEPES, 4 mM Na_2ATP, 0.06 mM spermine, adjusted to 310 mOsm, and pH 7.2 with CsOH. Pipette resistance was 2–4 MΩ. After a whole-cell recording was achieved, the cell was gently pulled and lifted off the coverslip and placed under the flow of a theta tube. Fast application was achieved by moving the theta tube laterally with a piezoelectric device (Burleigh). Glutamate (1 mM) was applied every 20 to 30 s. Cells were kept at –40 mV. I-V curves were obtained by stepping the voltage 100 ms before the glutamate application.

Electrophysiological Recordings of Neurons

Primary cultures of hippocampal neurons were prepared from wild-type or $GluR5^{-/-}$ × $GluR6^{-/-}$ mice. For transfection of neurons, we used Lipofectamine 2000 to cotransfect untagged GluR6 subunits and GFP at a ratio of 2:1 (one subunit) or 1:1:1 (two subunits). Neurons were transfected 7–8 days after plating, and recorded 1 to 4 days after transfection. Overall, neurons were recorded 7–15 days after plating. Cells were bathed in HBS at room temperature, and under the flow of a three-barrel pipette containing HBS without $MgCl_2$, which contained 1 μM TTX, 100 μM GYKI 53655, 50 μM picrotoxine, and 2 μM glycine. One of the barrels contained, in addition, 200 μM NMDA, and another, 300 μM kainate. Kainate was applied for 1 s every minute. To test for KAR depression by NMDAR activation, NMDA was applied for 3 s, at intervals of 2 s, 4 s, or 8 s before kainate. Recording pipettes contained 141 mM CsCl, 2 mM NaCl, 2 mM $MgCl_2$, 0.5 mM EGTA, 10 mM HEPES, and 4 mM Na_2ATP. In some experiments, EGTA was replaced by 10 mM BAPTA. In other experiments, 100 μM of peptides corresponding to the last 15 amino acids of GluR6b or to a 15 amino acid scrambled sequence (H_2N-KSWPHTDPSIYVLEPVC-$CONH_2$) was added, together with a cocktail of antiproteases (pepstatin, aprotinin, leupeptin, and pefabloc [10 μg/ml each]).

Preparation of Brain Protein Extract

For each experiment, proteins from three mouse brains were extracted and solubilized by 1% Triton X-100 as in Coussen et al. (2002). The resulting supernatant was the Triton X-100 extract used for immunoprecipitation experiments.

Immunoprecipitation

Myc-GluR6 proteins were immunoprecipitated from αCaMKIIa-myc-GluR6 transgenic lines, as previously described (Coussen et al., 2002). The anti-myc antibody was linked to protein-G agarose with 20 mM dimethyl pimelimidate during 30 min at room temperature. Immunoprecipitated proteins were eluted with either 350 μl isoelectrofocusing medium (7 M urea, 2 M thiourea, 4% CHAPS, ampholines [preblended, pI, 3.5–9.5, 8 mg/ml; Amersham Biosciences], 100 mM DTT, 0.2% tergitol NP7 [Sigma], and traces of bromophenol blue), for two-dimensional (2D) electrophoresis, or 100 μl SDS sample buffer (50 mM Tris-HCl [pH, 6.8], 2% SDS, 10% glycerol, 100 mM DTT, and traces of bromophenol blue), for immunoblotting.

Peptide Affinity Chromatography

Affinity chromatography experiments were performed using either the entire GluR6a C-terminal domain (70 amino acids) fused to GST (GST-GluR6a pull-down) or the synthetic GluR6b peptide. This peptide was coupled via its N-terminal extremity to activated CH-Sepharose 4B (Amersham Biosciences), according to the manufacturer's instructions. Cytosolic protein extracts from mice brain (6 mg) were incubated with either GST-GluR6a, GST (5 mg each) or GluR6b C-terminal peptide (2 mg). For bidimensional analysis, proteins were eluted with reduced glutathione (10 mM), precipitated with 10% trichloroacetic acid, and solubilized in isoelectrofocusing medium. For Western blot analysis, GST samples were resuspended in SDS sample buffer. In competition assays, R6b or scramble peptides were incubated during the reaction at concentrations indicated in the figure.

Two-Dimensional Electrophoresis and Identification of Proteins by MALDI-TOF Mass Spectrometry

Proteins were first separated according to their isoelectric point along linear immobilized pH-gradient (IPG) strips (pH, 3–10, 18 cm long; Amersham Biosciences). Sample loading for the first dimension was performed by passive in-gel reswelling. The IPG strips were then equilibrated for 10 min in a buffer containing 6M urea, 50 mM Tris-HCl (pH, 6.8), 30% glycerol, 2% SDS, 10 mg/ml DTT, and bromophenol blue and then equilibrated for 15 min in the same buffer containing 15 mg/ml iodoacetamide instead of the DTT. For the second dimension, the strips were loaded onto vertical 12.5% SDS polyacrylamide gels. Gels were silver stained (Shevchenko et al., 1996). Gels to be compared were always processed and stained in parallel. Gels were scanned using a computer-assisted densitometer (Amersham). Spot detection, gel alignment, background substraction, and spot quantification were performed with the Melanie 5 software (Amersham), using four gels for each experimental condition. To correct for variability resulting from silver staining, total spot volume normalization was performed after background substraction for each gel.

Protein spots that were not detected in control gels were excised and digested in gel using trypsin (Promega). Digest products were loaded onto the target of an Ultraflex MALDI-TOF mass spectrometer (Bruker-Franzen Analytik) and mixed with the same volume of α-cyano-4-hydroxy-*trans*-cinnamic acid (10 mg/ml in acetonitrile-TFA, 50%–0.1%; Sigma). Analysis was performed in reflectron mode with an accelerating voltage of 20 kV and a delayed extraction of 400 ns. Spectra were analyzed using the XTOF software (Bruker-Franzen Analytik) and auto-proteolysis products of trypsin (M_r: 842.51, 1045.56, 2211.10) were used as internal calibrates. Identification of proteins was performed using the Mascot software (available online at http://www.matrixscience.com), as previously described (Becamel et al., 2002).

Surface Biotinylation

One day after transfection, COS-7 cells were washed with PBS (pH, 8.0) and incubated with 0.5 mg/ml of EZ-Link Sulfo-NHS-S-LC-Biotin (Pierce) in PBS for 30 min at 4°C. Cells were scraped in lysis buffer containing 25 mM HEPES, 150 mM NaCl, 1% Triton X-100, and protease inhibitors. After centrifugation, the supernatant was incubated with immobilized Streptavidin beaded agarose overnight at 4°C and extensively washed. Samples were analyzed by Western blot with antibodies corresponding to the proteins of interest.

Antibodies

The sources of antibodies used were: Anti-GluR6a/GluR7 (06-309), anti-KA2 (06-315), anti-myc polyclonal (06-549), anti-calmodulin (05-173), and anti-Dynamin-1 (05-319), from Upstate; anti-calcineurin (AB-1694), from Chemicon; anti-myc monoclonal (1 667 149), from Roche; anti-14-3-3 (sc-731), from Santa Cruz; anti-spectrin (S 3396), from Sigma; and anti-NSF (123 002), from Synaptic Systems; anti-F3-contactin, the gift of C. Faivre Sarrailh; anti-profilin II, the gift of W. Witke; and anti-VILIP 1 and anti-VILIP 3, the gift of D. Ladant. GluR6b antibodies (Seraing) were produced as described above.

Acknowledgments

This work was supported by grants from the Centre National de la Recherche Scientifique, the Ministère de la Recherche of France, the Conseil Régional d'Aquitaine, the European Commission (contract QLRT-2000-02089), the Fondation pour la Recherche Médi-

cale (to D.P.), the French Foreign Ministry (to S.S.), and Proteom platform of Monpellier Genopole.

Received: December 20, 2004
Revised: May 26, 2005
Accepted: June 29, 2005
Published: August 17, 2005

References

Ackermann, M., and Matus, A. (2003). Activity-induced targeting of profilin and stabilization of dendritic spine morphology. Nat. Neurosci. *6*, 1194–1200.

Ayalon, G., and Stern-Bach, Y. (2001). Functional assembly of AMPA and kainate receptors is mediated by several discrete protein-protein interactions. Neuron *31*, 103–113.

Barry, M.F., and Ziff, E.B. (2002). Receptor trafficking and the plasticity of excitatory synapses. Curr. Opin. Neurobiol. *12*, 279–286.

Becamel, C., Alonso, G., Galeotti, N., Demey, E., Jouin, P., Ullmer, C., Dumuis, A., Bockaert, J., and Marin, P. (2002). Synaptic multiprotein complexes associated with 5-HT(2C) receptors: a proteomic approach. EMBO J. *21*, 2332–2342.

Becamel, C., Gavarini, S., Chanrion, B., Alonso, G., Galeotti, N., Dumuis, A., Bockaert, J., and Marin, P. (2004). The serotonin 5–HT2A and 5–HT2C receptors interact with specific sets of PDZ proteins. J. Biol. Chem. *279*, 20257–20266.

Berg, D., Holzmann, C., and Riess, O. (2003). 14-3-3 proteins in the nervous system. Nat. Rev. Neurosci. *4*, 752–762.

Bernard, V., Normand, E., and Bloch, B. (1992). Phenotypical characterization of the rat striatal neurons expressing muscarinic receptor genes. J. Neurosci. *12*, 3591–3600.

Bettler, B., and Mulle, C. (1995). AMPA and kainate receptors. Neuropharmacology *34*, 123–139.

Bortolotto, Z.A., Clarke, V.R., Delany, C.M., Parry, M.C., Smolders, I., Vignes, M., Ho, K.H., Miu, P., Brinton, B.T., Fantaske, R., et al. (1999). Kainate receptors are involved in synaptic plasticity. Nature *402*, 297–301.

Bowie, D., and Mayer, M.L. (1995). Inward rectification of both AMPA and kainate subtype glutamate receptors generated by polyamine-mediated ion channel block. Neuron *15*, 453–462.

Braithwaite, S.P., Xia, H., and Malenka, R.C. (2002). Differential roles for NSF and GRIP/ABP in AMPA receptor cycling. Proc. Natl. Acad. Sci. USA *99*, 7096–7101.

Bredt, D.S., and Nicoll, R.A. (2003). AMPA receptor trafficking at excitatory synapses. Neuron *40*, 361–379.

Burgoyne, R.D., and Weiss, J.L. (2001). The neuronal calcium sensor family of Ca2+-binding proteins. Biochem. J. *353*, 1–12.

Carroll, R.C., Beattie, E.C., Xia, H., Luscher, C., Altschuler, Y., Nicoll, R.A., Malenka, R.C., and von Zastrow, M. (1999). Dynamin-dependent endocytosis of ionotropic glutamate receptors. Proc. Natl. Acad. Sci. USA *96*, 14112–14117.

Chazot, P.L., and Stephenson, F.A. (1997). Molecular dissection of native mammalian forebrain NMDA receptors containing the NR1 C2 exon: direct demonstration of NMDA receptors comprising NR1, NR2A, and NR2B subunits within the same complex. J. Neurochem. *69*, 2138–2144.

Choquet, D., and Triller, A. (2003). The role of receptor diffusion in the organization of the postsynaptic membrane. Nat. Rev. Neurosci. *4*, 251–265.

Collingridge, G.L., Isaac, J.T., and Wang, Y.T. (2004). Receptor trafficking and synaptic plasticity. Nat. Rev. Neurosci. *5*, 952–962.

Contractor, A., Swanson, G., and Heinemann, S.F. (2001). Kainate receptors are involved in short- and long-term plasticity at mossy fiber synapses in the hippocampus. Neuron *29*, 209–216.

Contractor, A., Sailer, A.W., Darstein, M., Maron, C., Xu, J., Swanson, G.T., and Heinemann, S.F. (2003). Loss of kainate receptor-mediated heterosynaptic facilitation of mossy-fiber synapses in KA2–/– mice. J. Neurosci. *23*, 422–429.

Coussen, F., Normand, E., Marchal, C., Costet, P., Choquet, D., Lambert, M., Mege, R.M., and Mulle, C. (2002). Recruitment of the kainate receptor subunit glutamate receptor 6 by cadherin/catenin complexes. J. Neurosci. *22*, 6426–6436.

Cui, C., and Mayer, M.L. (1999). Heteromeric kainate receptors formed by the coassembly of GluR5, GluR6, and GluR7. J. Neurosci. *19*, 8281–8291.

Da Silva, J.S., Medina, M., Zuliani, C., Di Nardo, A., Witke, W., and Dotti, C.G. (2003). RhoA/ROCK regulation of neuritogenesis via profilin IIa-mediated control of actin stability. J. Cell Biol. *162*, 1267–1279.

Ehlers, M.D., Zhang, S., Bernhadt, J.P., and Huganir, R.L. (1996). Inactivation of NMDA receptors by direct interaction of calmodulin with the NR1 subunit. Cell *84*, 745–755.

Garcia, E.P., Mehta, S., Blair, L.A., Wells, D.G., Shang, J., Fukushima, T., Fallon, J.R., Garner, C.C., and Marshall, J. (1998). SAP90 binds and clusters kainate receptors causing incomplete desensitization. Neuron *21*, 727–739.

Ghetti, A., and Heinemann, S.F. (2000). NMDA-dependent modulation of hippocampal kainate receptors by calcineurin and Ca(2+)/calmodulin-dependent protein kinase. J. Neurosci. *20*, 2766–2773.

Gray, N.W., Fourgeaud, L., Huang, B., Chen, J., Cao, H., Oswald, B.J., Hemar, A., and McNiven, M.A. (2003). Dynamin 3 is a component of the postsynapse, where it interacts with mGluR5 and Homer. Curr. Biol. *13*, 510–515.

Hirbec, H., Francis, J.C., Lauri, S.E., Braithwaite, S.P., Coussen, F., Mulle, C., Dev, K.K., Couthino, V., Meyer, G., Isaac, J.T., et al. (2003). Rapid and differential regulation of AMPA and kainate receptors at hippocampal mossy fibre synapses by PICK1 and GRIP. Neuron *37*, 625–638.

Huettner, J.E. (2003). Kainate receptors and synaptic transmission. Prog. Neurobiol. *70*, 387–407.

Jaskolski, F., Coussen, F., Nagarajan, N., Normand, E., Rosenmund, C., and Mulle, C. (2004). Subunit composition and alternative splicing regulate membrane delivery of kainate receptors. J. Neurosci. *24*, 2506–2515.

Jaskolski, F., Coussen, F., and Mulle, C. (2005). Subcellular localization and trafficking of kainate receptors. Trends Pharmacol. Sci. *26*, 20–26.

Lee, S.H., Simonetta, A., and Sheng, M. (2004). Subunit rules governing the sorting of internalized AMPA receptors in hippocampal neurons. Neuron *43*, 221–236.

Lerma, J. (2003). Roles and rules of kainate receptors in synaptic transmission. Nat. Rev. Neurosci. *4*, 481–495.

Lin, L., Jeanclos, E.M., Treuil, M., Braunewell, K.H., Gundelfinger, E.D., and Anand, R. (2002). The calcium sensor protein visinin-like protein-1 modulates the surface expression and agonist sensitivity of the alpha 4beta 2 nicotinic acetylcholine receptor. J. Biol. Chem. *277*, 41872–41878.

Man, H.Y., Lin, J.W., Ju, W.H., Ahmadian, G., Liu, L., Becker, L.E., Sheng, M., and Wang, Y.T. (2000). Regulation of AMPA receptor-mediated synaptic transmission by clathrin-dependent receptor internalization. Neuron *25*, 649–662.

Mu, Y., Otsuka, T., Horton, A.C., Scott, D.B., and Ehlers, M.D. (2003). Activity-dependent mRNA splicing controls ER export and synaptic delivery of NMDA receptors. Neuron *40*, 581–594.

Mulle, C., Andreas, S., Pérez-Otaño, I., Dickinson-Anson, H., Castillo, P.E., Bureau, I., Maron, C., Gage, F.H., Mann, J.R., Bettler, B., and Heinemann, S.F. (1998). Altered synaptic physiology and reduced susceptibility to kainate induced seizures in GluR6-deficient mice. Nature *392*, 601–604.

Mulle, C., Sailer, A., Swanson, G.T., Brana, C., O'Gorman, S., Bettler, B., and Heinemann, S.F. (2000). Subunit composition of kainate receptors in hippocampal interneurons. Neuron *28*, 475–484.

Nishimune, A., Isaac, J.T., Molnar, E., Noel, J., Nash, S.R., Tagaya, M., Collingridge, G.L., Nakanishi, S., and Henley, J.M. (1998). NSF binding to GluR2 regulates synaptic transmission. Neuron *21*, 87–97.

Nong, Y., Huang, Y.Q., Ju, W., Kalia, L.V., Ahmadian, G., Wang, Y.T., and Salter, M.W. (2003). Glycine binding primes NMDA receptor internalization. Nature *422*, 302–307.

Nourry, C., Grant, S.G., and Borg, J.P. (2003). PDZ domain proteins: plug and play! Sci. STKE *179*, RE7.

O'Kelly, I., Butler, M.H., Zilberberg, N., and Goldstein, S.A. (2002). Forward transport. 14-3-3 binding overcomes retention in endoplasmic reticulum by dibasic signals. Cell *111*, 577–588.

Paternain, A.V., Herrera, M.T., Nieto, M.A., and Lerma, J. (2000). GluR5 and GluR6 kainate receptor subunits coexist in hippocampal neurons and coassemble to form functional receptors. J. Neurosci. *20*, 196–205.

Ren, Z., Riley, N.J., Garcia, E.P., Sanders, J.M., Swanson, G.T., and Marshall, J. (2003a). Multiple trafficking signals regulate kainate receptor KA2 subunit surface expression. J. Neurosci. *23*, 6608–6616.

Ren, Z., Riley, N.J., Needleman, L.A., Sanders, J.M., Swanson, G.T., and Marshall, J. (2003b). Cell surface expression of GluR5 kainate receptors is regulated by an endoplasmic reticulum retention signal. J. Biol. Chem. *278*, 52700–52709.

Schroer, T.A. (2004). Dynactin. Annu. Rev. Cell Dev. Biol. *20*, 759–779.

Sever, S. (2002). Dynamin and endocytosis. Curr. Opin. Cell Biol. *14*, 463–467.

Sheng, M. (2001). Molecular organization of the postsynaptic specialization. Proc. Natl. Acad. Sci. USA *98*, 7058–7061.

Sheng, M., Cummings, J., Roldan, L.A., Jan, Y.N., and Jan, L.Y. (1994). Changing subunit composition of heteromeric NMDA receptors during development of rat cortex. Nature *368*, 144–147.

Shevchenko, A., Wilm, M., Vorm, O., and Mann, M. (1996). Mass spectrometric sequencing of proteins silver-stained polyacrylamide gels. Anal. Chem. *68*, 850–858.

Song, I., and Huganir, R.L. (2002). Regulation of AMPA receptors during synaptic plasticity. Trends Neurosci. *25*, 578–588.

Song, I., Kamboj, S., Xia, J., Dong, H., Liao, D., and Huganir, R.L. (1998). Interaction of the N-ethylmaleimide-sensitive factor with AMPA receptors. Neuron *21*, 393–400.

Spilker, C., and Braunewell, K.H. (2003). Calcium-myristoyl switch, subcellular localization, and calcium-dependent translocation of the neuronal calcium sensor protein VILIP-3, and comparison with VILIP-1 in hippocampal neurons. Mol. Cell. Neurosci. *24*, 766–778.

Tashiro, A., Dunaevsky, A., Blazeski, R., Mason, C.A., and Yuste, R. (2003). Bidirectional regulation of hippocampal mossy fiber filopodial motility by kainate receptors: a two-step model of synaptogenesis. Neuron *38*, 773–784.

Traynelis, S.F., and Wahl, P. (1997). Control of rat GluR6 glutamate receptor open probability by protein kinase A and calcineurin. J. Physiol. *503*, 513–531.

Vallee, R.B., Williams, J.C., Varma, D., and Barnhart, L.E. (2004). Dynein: An ancient motor protein involved in multiple modes of transport. J. Neurobiol. *58*, 189–200.

Wang, L.Y., Taverna, F.A., Huang, X.P., MacDonald, J.F., and Hampson, D.R. (1993). Phosphorylation and modulation of a kainate receptor (GluR6) by cAMP-dependent protein kinase. Science *259*, 1173–1175.

Wang, Y.T., and Linden, D.J. (2000). Expression of cerebellar long-term depression requires postsynaptic clathrin-mediated endocytosis. Neuron *25*, 635–647.

Wechsler, A., and Teichberg, V.I. (1998). Brain spectrin binding to the NMDA receptor is regulated by phosphorylation, calcium and calmodulin. EMBO J. *17*, 3931–3939.

Wenthold, R.J., Trumpy, V.A., Zhu, W.S., and Petralia, R.S. (1994). Biochemical and assembly properties of GluR6 and KA2, two members of the kainate receptor family, determined with subunit-specific antibodies. J. Biol. Chem. *269*, 1332–1339.

Wenthold, R.J., Prybylowski, K., Standley, S., Sans, N., and Petralia, R.S. (2003). Trafficking of NMDA receptors. Annu. Rev. Pharmacol. Toxicol. *43*, 335–358.

Winder, D.G., and Sweatt, J.D. (2001). Roles of serine/threonine phosphatases in hippocampal synaptic plasticity. Nat. Rev. Neurosci. *2*, 461–474.

Witke, W., Podtelejnikov, A.V., Di Nardo, A., Sutherland, J.D., Gurniak, C.B., Dotti, C., and Mann, M. (1998). In mouse brain profilin I and profilin II associate with regulators of the endocytic pathway and actin assembly. EMBO J. *17*, 967–976.

Yan, S., Sanders, J.M., Xu, J., Zhu, Y., Contractor, A., and Swanson, G.T. (2004). A C-terminal determinant of GluR6 kainate receptor trafficking. J. Neurosci. *24*, 679–691.

Yuan, H., Michelsen, K., and Schwappach, B. (2003). 14-3-3 dimers probe the assembly status of multimeric membrane proteins. Curr. Biol. *13*, 638–646.

Zukin, R.S., and Bennett, M.V. (1995). Alternatively spliced isoforms of the NMDARI receptor subunit. Trends Neurosci. *18*, 306–313.